Microring Resonators Vertically Coupled to Buried Heterostructure Bus Waveguides

Seung June Choi, Kostadin Djordjev, Sang Jun Choi, P. Daniel Dapkus, *Fellow, IEEE*, Wilson Lin, Giora Griffel, Ray Menna, and John Connolly

Abstract—The authors demonstrate all epitaxial semiconductor microring resonators vertically coupled to buried heterostructure (BH) bus waveguides for the first time. Planar vertically stacked waveguides are successfully grown on BH mesas by conducting a two-step regrowth process. This approach is potentially important for any buried waveguide technology where subsequent surface planarity is required. The measured transmission spectra show resonance dips $(1.55 \sim 1.60)$ μm with quality factors, extinction ratios, and free spectral ranges of $2500 -3.5$ dB, and ~ 11 nm, respectively, for 10-μm-radii microrings.

Index Terms—Buried heterostructure (BH), epitaxial regrowth, extinction ratio, free spectral range, microresonator, microring, quality factor.

I. INTRODUCTION

CIRCULAR microresonator wavelength add–drop filters have been of great interest in dense wavelength-division multiplexing (DWDM) applications due to their small feature size (radius < 15 μm), narrow linewidth, and large free spectral range (FSR). In actual add–drop filter configurations, the microresonator is either laterally [1] or vertically [2] coupled to the input/output (I/O) bus waveguides. The vertical geometry is advantageous because the material compositions and physical separation of the I/O bus and the resonator layer can be independently designed and controlled. This facilitates the design and fabrication of active devices with precisely controlled characteristics such as coupling efficiency, resonance wavelength, bandwidth, and so on.

Recently, three-dimensional (3-D) vertically coupled microresonators have been produced by utilizing a wafer bonding technology that usually requires a direct thermal fusion method [2] or a polymer bonding layer [3]. Although wafer bonding is quite successful, an all-epitaxial technology without wafer bonding for vertically coupled microresonators on buried I/O buses is attractive. The buried bus design would serve as a robust platform and provide the needed conductive and thermal paths to the substrate for active microresonators. The microresonators in such a device must lie on top, and in close proximity to the bus waveguides to enable the fabrication of small radius air-guided structures. In such structures, the planarity of the waveguiding layers comprising the microresonator is crucial

for minimizing scattering loss and maintaining the required Q factor. Even a minute undulation in the surface on which the ring is fabricated might lead to detrimental effects on its performance. A similar buried bus design has been realized in microrings using glass materials [4], but it has not been successful for semiconductors to date due to the difficulty in epitaxial growth. It is extremely difficult to planarize layers regrown on mesas or rib-type waveguides within the very short distance required for optical coupling using conventional metalorganic chemical vapor deposition (MOCVD). In practice, the irregularity of the initial surface is reproduced throughout the layers in the regrowth process up to a thickness of a few microns. Therefore, a method for planarization of buried heterostructure (BH) waveguiding channels with excellent uniformity across the wafer and regrowth of additional waveguiding layers within a close proximity is required.

In this letter, microring resonators vertically coupled to BH bus waveguides are demonstrated. A carefully engineered two-step regrowth process is utilized to realize a planar waveguide on top of buried mesas. We then follow to process thin linewidth (~ 1 μm), small radius (~ 10 μm) ring resonators from the planar waveguide. A thin microring design is favorable, compared with a microdisk, to suppress the optical interaction of higher order radial modes in the resonator-bus coupling process. The suggested approach takes full advantage of vertically coupled microresonators using all-epitaxial fabrication demonstrating excellent planarity without having to resort to the wafer-bonding technique.

II. EXPERIMENTS

A Thomas Swan low-pressure MOCVD (LP-MOCVD) system equipped with a vertical closed space showerhead reactor was used for the material growth in this study. To initiate the process, a 0.4-μm-thick InGaAsP ($\lambda_{\text{Bus}} = 1.1$ μm) bus waveguide layer is grown on an (001)-oriented InP substrate and covered by a 0.1-μm-thick SiN_x layer deposited as a masking layer. Stripe I/O bus patterns are defined and etched into this layer along the [110] direction using contact photolithography and CH_4-based reactive ion etching (RIE) as shown in Fig. 1(a). The resultant mesas are 1 μm wide, having vertical sidewalls as steep as $87°$. Once the waveguides to be buried are formed, the polymers generated on the sidewalls during the dry-etching process are cleaned by an oxygen plasma treatment. The SiN_x mask is left on the mesa for the first InP regrowth step that is done to fill the empty regions between the mesas, Fig. 1(b). The V/III ratio was varied from 340 to 240 to determine the effect of the PH_3 partial pressure on the regrowth behavior

Report Documentation Page

1. REPORT DATE	2. REPORT TYPE	3. DATES COVERED
01 JUN 2005	**N/A**	**-**

4. TITLE AND SUBTITLE	5a. CONTRACT NUMBER
Microring Resonators Vertically Coupled to Buried Heterostructure Bus Waveguides	5b. GRANT NUMBER
	5c. PROGRAM ELEMENT NUMBER

6. AUTHOR(S)	5d. PROJECT NUMBER
	5e. TASK NUMBER
	5f. WORK UNIT NUMBER

7. PERFORMING ORGANIZATION NAME(S) AND ADDRESS(ES)	8. PERFORMING ORGANIZATION REPORT NUMBER
Department of Electrical Engineering-Electrophysics, University of Southern California, Los Angeles, CA 90089 USA	

9. SPONSORING/MONITORING AGENCY NAME(S) AND ADDRESS(ES)	10. SPONSOR/MONITOR'S ACRONYM(S)
	11. SPONSOR/MONITOR'S REPORT NUMBER(S)

12. DISTRIBUTION/AVAILABILITY STATEMENT
Approved for public release, distribution unlimited

13. SUPPLEMENTARY NOTES
See also ADM001923.

14. ABSTRACT

15. SUBJECT TERMS

16. SECURITY CLASSIFICATION OF:			17. LIMITATION OF ABSTRACT	18. NUMBER OF PAGES	19a. NAME OF RESPONSIBLE PERSON
a. REPORT **unclassified**	b. ABSTRACT **unclassified**	c. THIS PAGE **unclassified**	**UU**	**3**	

while the growth temperature was maintained at 690 °C. Low V/III ratio is preferable to avoid a sloped overgrowth along the dry-etched mesas, since it enhances the surface migration of the group-III species. However, voids appeared along the mesa sidewalls when the V/III ratio was lower than 280. The best planarized wafer is obtained from samples that were filled with InP at V/III $=$ 291. The SiN_x layer was removed by a buffered oxide etchant (BOE) after the first regrowth step. The second regrowth is to build vertically stacked layers on the buried mesas as depicted in Fig. 1(c). A 0.4-μm-thick InGaAsP (λ_{Ring} $=$ 1.4 μm) waveguide, sandwiched by a 0.8-μm-thick coupling and a 1.0-μm-thick top cladding InP layers, is grown on the BH buses to produce the vertically coupled waveguide structure. The specific high-index resonator waveguide core material is chosen as a compromise between the need to phase-match the bus and resonator waveguides while maintaining low absorption loss in the resonator. The effective indexes of the microring and the BH bus waveguides must be matched closely enough to provide sufficient power coupling, while the material loss in the spectral range of interest ($\lambda = 1.55 \sim 1.60$ μm) should be maintained as low as possible. The effective indexes of each waveguide will be discussed again in Section III of this letter. The subsequent epitaxial structures are quite planar as shown in Fig. 2.

In order to make the BH buses visible for the following microring alignment process, we selectively remove the top layers along the substrate edge by using wet etching solutions. After microring patterns are defined lithographically, very smooth microring mesas are formed on the planarized wafer surface by using CH_4-based chemistries in an RIE discharge [5]. The typical ring radius and linewidth are 10 and 1 μm, respectively. Fig. 3 shows the microring produced on BH waveguides. Note the apparent perfect planarity of the ring as it travels across the boundary of the BH bus channels. The resultant etch profile is slightly sloped, which may cause polarization in the resonator. The ring mesa is etched ~ 2 μm deep, leaving a thin ($\sim$ 0.2 μm), nearly electron-transparent InP membrane on the BH buses. The wafer is mechanically thinned and bars are cleaved 600 μm long for the measurement. Finally, the antireflection (AR) coating is deposited on both facets to suppress undesired Fabry–Pérot resonance from the bus waveguides.

III. RESULTS AND DISCUSSIONS

The resonant characteristics of 10-μm-radii microrings are measured as a wavelength drop filter by exciting one of the buried I/O bus facets with an out-of-wafer-plane TE-polarized tunable (1.54 $\sim$ 1.61 μm) external cavity laser diode and collecting the transmitted power at the other end. The normalized measured transmission spectra are given in Fig. 4. A clear sign of resonance is observed over a wide spectral range, indicating the successful planarized regrowth technology on BH bus waveguides. Typical quality factors (Qs), extinction ratios, and FSRs are 2500, −3.5 dB, and ∼11 nm, respectively, from which finess (F) of ∼18 is estimated. The observed F is inferior to recent state-of-the-art values (typically 40 or greater), mainly due to the high optical losses observed in the measured devices.

InP InGaAsP for rings SiN
InGaAsP for bus waveguides
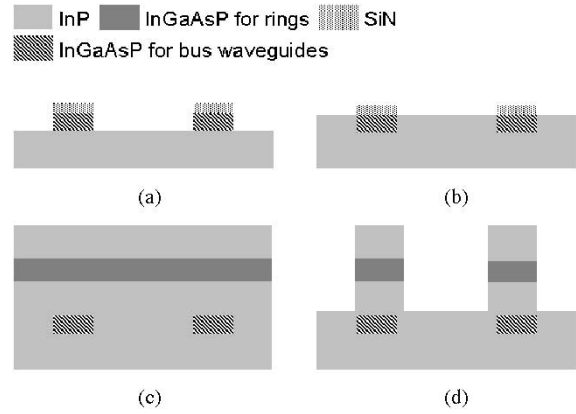
(a)   (b)

(c)   (d)

Fig. 1. Schematic drawings showing the process flow to fabricate microring resonators vertically coupled to buried heterostructure bus waveguides. (a) Dry-etched bus waveguides, (b) the first regrowth to fill the empty region between the dry-etched mesas, (c) the second regrowth process to have vertically stacked waveguides, and (d) microring formation on the buried bus waveguides, respectively.
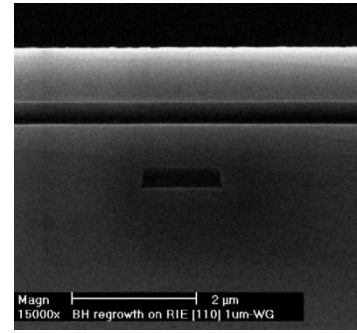

Fig. 2. Scanning-electron microscopic (SEM) image of the cross section of a planar vertically stacked waveguide produced on BH mesas by conducting a two-step regrowth process. Structure shown in this picture corresponds to the process Fig. 1(c). Waveguide materials are selectively stain-etched for contrasts.
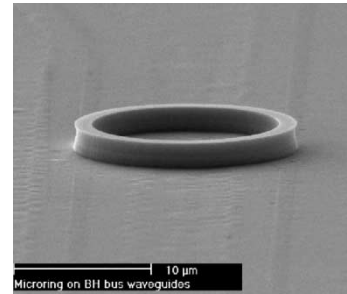

Fig. 3. SEM image of a microring resonator vertically coupled to buried bus waveguides. 10-μm-radius microring is shown in this picture.

The fabricated resonators are numerically characterized as follows. First, effective index approximation is combined with a conformal transformation to calculate the effective mode indexes of the microring and the buried bus waveguides, respectively. For the given device structure, $n_{eff,Ring}$ $=$ 3.157 and $n_{eff,Bus}$ $=$ 3.168 are obtained. Then, the modal field distribution in the ring and the bus waveguides are computed by a finite difference (FD) method, from which local coupling coefficients can be calculated by solving the overlap integral of the fields and the effective index distribution [6]. Finally, the overall power coupling (κ) is calculated by integrating the coupled-mode equations (CMEs) with respect to the propagation distance in the bus waveguides. The fifth-
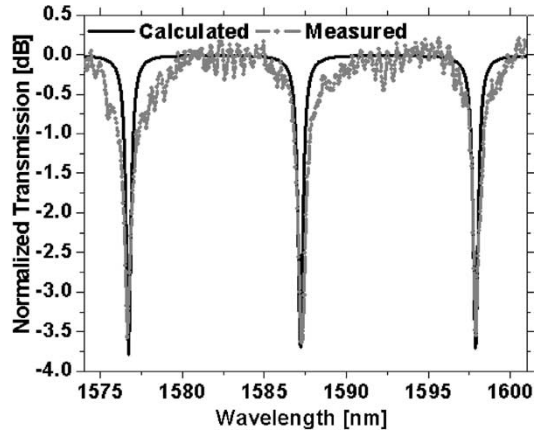
Fig. 4. Measured and calculated transmission spectra for a 10-μm-radius microring resonator. TE-polarized input light is coupled into the input bus waveguide. For the calculated spectra, $R = 10.1\ \mu$m, $n_{\text{eff,Ring}} = 3.157$, $\kappa_{\text{in}} = 4.5\%$, $\kappa_{\text{out}} = 4.0\%$, and $\alpha = 20\ \text{cm}^{-1}$ are used to fit the measured data.

order Runge–Kutta method [7] is employed to solve the differential CMEs. The power-coupling coefficient is calculated to be $\kappa = 4.1\%$ for a TE-polarized input in the present device. The detailed calculation procedures for the given device geometries can be found in [8].

Waveguide-coupled microring resonators can be modeled in a similar way to Fabry–Pérot interferometers where the coupling junctions between the ring and the I/O buses form the mirrors. The reflectivity of the mirrors can be expressed by $R_1 = 1 - \kappa_{\text{in}}$ and $R_2 = 1 - \kappa_{\text{out}}$ for the input and output bus/ring couplers, respectively. Here, $\kappa_{\text{in,out}}$ denotes the power-coupling coefficient between the input and output waveguide and the ring. The normalized Lorentzian transmission characteristics T of a bus-coupled microring can be written as [9]

$$T = 1 - \frac{(1 - R_1)(1 - R_2 A^2)}{(1 - \sqrt{R_1 R_2} A)^2 + 4\sqrt{R_1 R_2} A \sin^2\left(\frac{\phi}{2}\right)}. \quad (1)$$

More details, the formalisms for bus-coupled microdisk resonators in particular, are described in [10]. The optical round trip path is l ($l = 2\pi r$ in case of circular resonators with radii of r), k_n is the wave vector, and α is the intensity attenuation coefficient or the total loss of the resonator. When (1) is used and the material dispersion is neglected, the best fit to the measured T is obtained at $r = 10.1\ \mu$m, $n_{\text{eff,Ring}} = 3.157$, $\kappa_{\text{in}} = 4.5\%$, $\kappa_{\text{out}} = 4.0\%$, and $\alpha = 20\ \text{cm}^{-1}$, respectively, as plotted in Fig. 4. The validity of the κ calculated in the previous paragraph is verified by the consistent fitting data for κ_{in} and κ_{out}. Probable fabrication errors, such as slight ring/bus misalignments and sloped ring sidewalls, can account for the asymmetric couplings and the enlarged ring radius in the fitting data. Our calculation suggests that a slight lateral offset of $\sim 0.15\ \mu$m may cause the observed difference in coupling coefficients of $\Delta\kappa = \kappa_{\text{in}} - \kappa_{\text{out}} \sim 0.5\%$.

The estimated loss for a TE-polarization input, $\alpha = 20\ \text{cm}^{-1}$, is several times greater than that of wafer-bonded microdisks vertically coupled to air-guided rib bus waveguides [2]. Since any imperfect boundary site on the inner and the outer sidewalls can scatter the energy of whispering gallery modes (WGMs)

to the radiation field, a thin-ring-type resonator usually has a higher scattering loss that contributes to the total loss. We also note that the present geometry affords weaker confinement of the WGM than air-supported structures, due to the smaller index step built along the vertical direction toward the substrate. Weak mode confinement leads to signal attenuation, due to leakage to the substrate [11]. A full vectorial computer-aided mode solver shows that the loss caused by mode leakage through the substrate becomes significant when the ring resonator core is not remote enough, $\sim 0.8\ \mu$m, or closer, from the planarized substrate. It is believed that using an index-matched design for the ring and the BH bus will diminish the substrate leakage loss, since the desired coupling coefficients can be obtained at larger separation between the ring and the bus waveguides under a phase-matched condition. According to our calculation, for example, $\kappa \sim 4\%$ is expected at 1.1 μm separation when the effective indexes are matched as $n_{\text{eff,Ring}} = n_{\text{eff,Bus}} = 3.168$. Further reduction of the substrate leakage can be afforded by designing large-radii (i.e., increasing the modal indexes) resonators, at the expense of smaller FSRs. A more attractive solution is to have the optical modes in resonators more securely isolated from a substrate by inserting a low-index medium underneath the resonator.

In conclusion, optical transmission of all-epitaxial InP–InGaAsP–InP microring resonators vertically coupled to BH bus waveguides is demonstrated for the first time. Planar vertically stacked waveguides are obtained on BH mesas by conducting a two-step regrowth process. This approach, envisioning 3-D construction of multiple semiconductor waveguides in PICs, is potentially important for any buried waveguide technology where subsequent surface planarity is required. The measured transmission spectra show Qs of 2500 and extinction ratios of -3.5 dB at resonance ($1.55 \sim 1.60\ \mu$m) for 10-μm-radii microrings. Further optimization should improve the device performance.

REFERENCES

[1] B. E. Little, S. T. Chu, H. A. Haus, J. Foresi, and J.-P. Laine, "Microring resonator channel dropping filters," *J. Lightwave Technol.*, vol. 15, pp. 998–1005, June 1997.

[2] D. V. Tishinin, I. Kim, C. Lin, A. E. Bond, and P. D. Dapkus, "Novel fabrication process for vertical resonant coupler with precise coupling efficiency," in *Proc. IEEE 11th Ann. LEOS Meeting*, Oct. 1998, pp. 93–94.

[3] R. Grover, P. P. Absil, V. Van, J. V. Hryniewicz, B. E. Little, O. King, L. C. Calhoun, F. G. Johnson, and P.-T. Ho, "Vertically coupled GaInAsP InP microring resonators," *Opt. Lett.*, vol. 26, pp. 506–508, Apr. 2001.

[4] B. E. Little, S. T. Chu, W. Pan, D. Ripin, T. Kaneko, Y. Kokubun, and E. Ippen, "Vertically coupled glass microring resonator channel dropping filters," *IEEE Photon. Technol. Lett.*, vol. 11, pp. 215–217, Feb. 1999.

[5] S. J. Choi, K. D. Djordjev, S. J. Choi, and P. D. Dapkus, "CH4-based dry etching of high Q InP microdisks," *J. Vac. Sci. Technol. B*, vol. 20, pp. 301–305, Jan. 2002.

[6] D. R. Rowland and J. D. Love, "Evanescent wave coupling of whispering gallery modes of a dielectric cylinder," *IEE Proc.*, vol. 140, no. 3, pp. 177–188, Mar. 1993.

[7] W. H. Press, B. P. Flannery, S. A. Teukolsky, and W. T. Vettering, *Numerical Recipes in C*. Cambridge, MA: Cambridge Univ. Press, 1988.

[8] K. D. Djordjev, Ph.D. dissertation, Univ. Southern California, USA, 2002.

[9] H. A. Haus, *Waves and Fields in Optoelectronics*. Englewood Cliffs, NJ: Prentice-Hall, 1984.

[10] D. G. Rabus, Ph.D. dissertation, Technischen Univ. Berlin, Germany, 2002.

[11] M. K. Chin and S. T. Ho, "Design and modeling of waveguide-coupled single-mode microring resonators," *J. Lightwave Technol.*, vol. 16, pp. 1433–1446, Aug. 1998.